



HAL
open science

Holocene Atmospheric Mercury Levels Reconstructed from Peat Bog Mercury Stable Isotopes

Maxime Enrico, Gaël Le Roux, Lars-Eric Heimbürger-Boavida, Pieter van Beek, Marc Souhaut, Jérôme Chmeleff, Jeroen E. Sonke

► **To cite this version:**

Maxime Enrico, Gaël Le Roux, Lars-Eric Heimbürger-Boavida, Pieter van Beek, Marc Souhaut, et al.. Holocene Atmospheric Mercury Levels Reconstructed from Peat Bog Mercury Stable Isotopes. Environmental Science and Technology, 2017, 51 (11), pp.5899-5906. 10.1021/acs.est.6b05804 . hal-02163109

HAL Id: hal-02163109

<https://hal.science/hal-02163109>

Submitted on 19 Mar 2024

HAL is a multi-disciplinary open access archive for the deposit and dissemination of scientific research documents, whether they are published or not. The documents may come from teaching and research institutions in France or abroad, or from public or private research centers.

L'archive ouverte pluridisciplinaire **HAL**, est destinée au dépôt et à la diffusion de documents scientifiques de niveau recherche, publiés ou non, émanant des établissements d'enseignement et de recherche français ou étrangers, des laboratoires publics ou privés.



Open Archive Toulouse Archive Ouverte

OATAO is an open access repository that collects the work of Toulouse researchers and makes it freely available over the web where possible

This is an author's version published in: <http://oatao.univ-toulouse.fr/20951>

Official URL:

<https://doi.org/10.1021/acs.est.6b05804>

To cite this version:

Enrico, Maxime^{ORCID} and Le Roux, Gaël^{ORCID} and Heimbürger, Lars-Éric^{ORCID} and Van Beek, Pieter^{ORCID} and Souhaut, Marc and Chmeleff, Jérôme^{ORCID} and Sonke, Jeroen^{ORCID} *Holocene Atmospheric Mercury Levels Reconstructed from Peat Bog Mercury Stable Isotopes*. (2017) *Environmental Science & Technology*, 51 (11). 5899-5906. ISSN 0013-936X

Any correspondence concerning this service should be sent to the repository administrator: tech-oatao@listes-diff.inp-toulouse.fr

Holocene Atmospheric Mercury Levels Reconstructed from Peat Bog Mercury Stable Isotopes

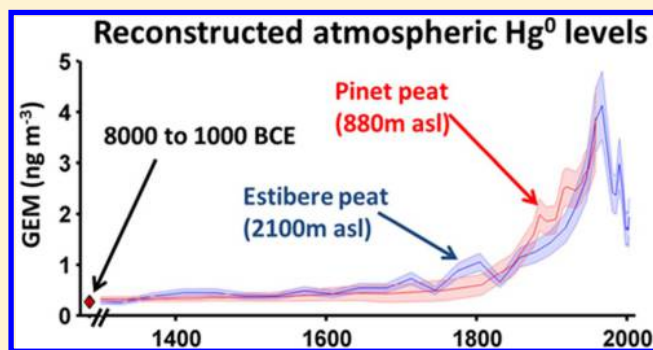
Maxime Enrico,^{*,†,‡,§} Gaël Le Roux,[†] Lars-Eric Heimbürger,^{‡,||} Pieter Van Beek,[§] Marc Souhaut,[§] Jérôme Chmeleff,[‡] and Jeroen E. Sonke^{*,‡,§}

[†]ECOLAB, Université de Toulouse, CNRS, INPT, UPS; ENSAT, Avenue de l'Agrobiopole, 31326 Castanet Tolosan, France

[‡]Laboratoire Géosciences Environnement Toulouse, Observatoire Midi-Pyrénées, CNRS/IRD/Université Paul Sabatier Toulouse III, 14 avenue Edouard Belin, 31400 Toulouse, France

[§]Laboratoire d'Études en Géophysiques et Océanographie, Observatoire Midi-Pyrénées, CNRS/IRD/Université Paul Sabatier Toulouse III, 14 avenue Edouard Belin, 31400 Toulouse, France

ABSTRACT: Environmental regulations on mercury (Hg) emissions and associated ecosystem restoration are closely linked to what Hg levels we consider natural. It is widely accepted that atmospheric Hg deposition has increased by a factor 3 ± 1 since preindustrial times. However, no long-term historical records of actual atmospheric gaseous elemental Hg (GEM) concentrations exist. In this study we report Hg stable isotope signatures in Pyrenean peat records (southwestern Europe) that are used as tracers of Hg deposition pathway ($\Delta^{200}\text{Hg}$, wet vs dry Hg deposition) and atmospheric Hg sources and cycling ($\delta^{202}\text{Hg}$, $\Delta^{199}\text{Hg}$). By anchoring peat-derived GEM dry deposition to modern atmospheric GEM levels we are able to reconstruct the first millennial-scale atmospheric GEM concentration record. Reconstructed GEM levels from 1970 to 2010 agree with monitoring data, and maximum 20th century GEM levels of $3.9 \pm 0.5 \text{ ng m}^{-3}$ were 15 ± 4 times the natural Holocene background of $0.27 \pm 0.11 \text{ ng m}^{-3}$. We suggest that a -0.7% shift in $\delta^{202}\text{Hg}$ during the medieval and Renaissance periods is caused by deforestation and associated biomass burning Hg emissions. Our findings suggest therefore that human impacts on the global mercury cycle are subtler and substantially larger than currently thought.



■ INTRODUCTION

The UNEP Minamata Convention aims at mitigating future human mercury exposure and restoring ecosystem mercury levels on a global scale.¹ Its success, by means of appropriate environmental regulations, depends in part on our perception of what environmental levels of mercury we consider natural. The historical impact of natural and anthropogenic atmospheric Hg emissions on deposition has been investigated using environmental archives such as ice cores,^{2,3} lake sediments,^{4–6} and peat bogs,^{7–9} but also by numerical modeling.^{10,11} Hg emissions, predominantly in the long-lived gaseous elemental Hg (GEM) form are slowly oxidized to more reactive divalent Hg species¹² that readily deposit to marine and terrestrial ecosystems.^{13–15} On the basis of shallow lake sediment archives it is widely accepted that atmospheric Hg deposition has increased by a factor 3 ± 1 since preindustrial times.^{5,13} Deeper lake sediment and peat archives probing the Holocene suggest a more pronounced increase in Hg deposition from prelarge scale mining times to present times by a factor of 17 to 27, respectively.¹¹ A global Hg box model also suggests large enrichment in atmospheric Hg, ranging from a factor 6 to 19

across different uncertainty scenarios.¹¹ In addition to the debate on historical Hg deposition, trends in Hg deposition may have a complex relationship to trends in atmospheric mercury concentrations and ultimately to atmospheric Hg emissions due to (i) the various forms of atmospheric Hg that may deposit, and (ii) the modulating effect of Hg's residence times in the atmosphere, oceans and critical zone.^{11,16} Past atmospheric mercury concentrations have thus far only been assessed by atmospheric monitoring since the 1970s¹⁷ and from glacier firn records ranging back to the 1940s.¹⁸ Both show a 2-fold decline since the 1970s.

Both sediment and peat bog records of past Hg deposition have long been thought to reflect Hg from wet deposition,^{8,19} with an additional influence of the watershed in the case of lake sediments. We recently examined the Hg isotope compositions of GEM and rainfall Hg at the ombrotrophic Pinet peat bog

(French Pyrenees) and compared them to living sphagnum moss and recently accumulated peat layers at Pinet.²⁰ A Hg isotope mass balance showed that Pinet sphagnum moss receives 80% of atmospheric Hg deposition by GEM sequestration (i.e., dry deposition, via a foliar uptake mechanism), and only 20% by wet deposition. We concluded that ombrotrophic sphagnum peat bogs are therefore potential archives of GEM dry deposition and of past GEM concentrations. Here we investigate for the first time the temporal evolution of GEM dry deposition, Hg wet deposition, and atmospheric GEM concentrations over the past 10 000 years using three cores from the Pinet peat bog and an additional core from Estibere peatland in the French Pyrenees (Figure S1 of the Supporting Information, SI).

METHODS

Study Sites. The Pinet peat bog (42.85°N, 1.97°E, 880 m a.s.l.) is located in the French Pyrenees (Figure S1). It is a 5 m-deep Sphagnum peat bog representing 10 000 years of peat accumulation. Annual precipitation in the area is 1161 mm (average for the period 2010–2014). The surface of the peat bog is at present sparsely covered by pine trees. Three 5 m-deep peat cores were sampled within a 10 m-radius in September 2010 using Wardenaar and Russian corers. An additional 72 cm-deep Wardenaar core was sampled in 2011 from the high altitude Estibere peatland (42.83°N, 0.17°E, 2120 m a.s.l.). Estibere is a minerotrophic sphagnum peatland located 150 km west to the Pinet peat bog (Figure S1). Both study sites are located in rural areas, far from any mine or industrial emission sources (>15 km).

Sample Preparation. Samples were prepared following Givélet et al.²¹ and Le Roux and De Vleeschouwer.²² The frozen peat cores were cut at 1 cm-resolution using a stainless steel band-saw. The edges of the samples were removed to avoid possible contamination during coring and storage, and kept frozen. Prior to analyses, peat samples were freeze-dried to avoid any loss of Hg. Pictures of every sample were taken and analyzed with ImageJ software in order to determine the surface of each slice and the thickness was measured. This method was chosen to precisely determine volume and density of samples, which is required to calculate Hg accumulation rates (HgAR).

Age Dating. ²¹⁰Pb, ¹³⁷Cs, and ²⁴¹Am activities were determined in 80 samples from the 3 Pinet peat cores and in 14 samples from the single Estibere peat core using the low-background gamma-spectrometers at the LAFARA underground laboratory of the Midi-Pyrenees Observatory²³ (Tables S1–S4 and Figures S2 and S3). The ²¹⁰Pb chronology for the last ~150 years was reconstructed assuming a constant rate of supply (CRS model).²⁴ Dating results are presented in detail in the SI (and Figures S4).

Six samples from Pinet core A were dated by the radiocarbon bomb pulse method. Sphagnum macrofossils (stem or leaves) were selected and measurements were done at the Laboratoire de Mesure du Carbone 14 (LMC14). Results are in good agreement with the ²¹⁰Pb CRS model (Figure S4) suggesting that both ²¹⁰Pb, and consequently Hg, were immobile.

Selected samples from the Pinet peat bog were measured for Pb stable isotope composition to validate the chronology inferred from ²¹⁰Pb CRS model (see Figures S5 and S6). A 100 mg aliquot of peat sample was digested using HNO₃/HF mixture and H₂O₂.²² They were then analyzed for Pb stable isotope composition using high resolution ICP-MS (Thermo-Element XR) at the Midi-Pyrenees Observatory (Toulouse,

France). Multiple analyses of a peat SRM (NIMT) prepared following the same protocol were used to estimate the reproducibility of the method. We found ²⁰⁶Pb/²⁰⁷Pb ratio of 1.176 ± 0.002 and ²⁰⁸Pb/²⁰⁶Pb of 2.094 ± 0.004 (1σ, n = 23), in good agreement with previous measurements.²⁵

On the basis of eight conventional ¹⁴C radiocarbon dates for the Pinet peat core and one radiocarbon date for the Estibere core, the ages of peat layers predating the industrial period were determined, including the early Holocene (Figure S7).

Hg Concentration Analyses. Total Hg concentrations in all peat samples (n = 342, 407, 377, and 51 for cores A, B, and C from the Pinet peat bog and the core from Estibere peatland, respectively) were measured by atomic absorption spectrophotometry (AAS) using a Milestone DMA-80. The instrument was calibrated with coal and lichen standard reference materials (SRMs NIST 1632d, NIST 2685b, and BCR 482). During analyses, coal or peat SRMs (NIST1632d, NIST2685b, NIMT) were measured every 15 samples to check the calibration, and procedural blanks were measured every 5 samples. NIST1632d, NIST2685b, and NIMT Hg concentration were 91.6 ± 8.2 ng g⁻¹ (1σ, n = 112), 144.7 ± 10.5 ng g⁻¹ (1σ, n = 73), and 157.9 ± 8.3 ng g⁻¹ (1σ, n = 22) respectively, for certified values of 92.8 ± 3.3, 146.2 ± 10.6, and 164 ± 20 ng g⁻¹. Duplicate Hg measurements were made on selected samples to assess reproducibility of the analyses (maximum of 10% variability for all duplicated samples).

Hg Extraction and Isotope Measurement. Selected peat samples were analyzed for Hg isotopic composition. The extraction procedure is detailed in Sun et al.²⁶ and briefly summarized here. A sample aliquot of 0.3 to 5 g was weighed and placed in a dual tube-furnace setup under a 25 mL min⁻¹ flow of Hg-free oxygen. The volatile sample combustion products, including gaseous Hg were transported from the first furnace into a second decomposition furnace kept at 1000 °C and then bubbled through a 40 vol % HNO₃/HCl (2:1) solution to oxidize and quantitatively trap gaseous Hg. The solutions were then diluted to 20 vol % acidity prior to isotopic composition analysis by cold vapor multicollector inductively coupled plasma mass spectrometry (CV-MC-ICPMS) at the Midi-Pyrenees Observatory (Toulouse, France). Hg recovery in the solutions ranged from 80 to 110%.

Measured Hg isotope ratios were corrected for instrumental mass bias by bracketing samples with the NIST SRM3133 standard. Delta values are expressed in permil (‰).²⁷

$$\delta^{xxx}\text{Hg} = \left(\frac{\left(\frac{^{xxx}\text{Hg}}{^{198}\text{Hg}} \right)_{\text{sample}}}{\left(\frac{^{xxx}\text{Hg}}{^{198}\text{Hg}} \right)_{\text{SRM3133}}} - 1 \right) \times 1000 \quad (1)$$

To quantify MIF, Δ-notation is used, and is the difference between the δ-value measured and the theoretical δ-value defined by mass-dependent fractionation:

$$\Delta^{xxx}\text{Hg} = \delta^{xxx}\text{Hg}_{\text{sample}} - \beta \times \delta^{202}\text{Hg}_{\text{sample}} \quad (2)$$

where β-values are 0.252, 0.502, 0.752, and 1.493 for isotopes 199, 200, 201, and 204, respectively, according to the kinetic MDF law.²⁷ Long-term expanded analytical uncertainties were assessed by replicate analyses of UM-Almaden and ETH Fluka SRMs. UM-Almaden displayed δ²⁰²Hg of -0.57 ± 0.06 ‰, Δ¹⁹⁹Hg of -0.03 ± 0.04 ‰, and Δ²⁰⁰Hg of 0.00 ± 0.04 ‰ (1σ, n = 46), and Fluka had δ²⁰²Hg of -1.43 ± 0.07 ‰, Δ¹⁹⁹Hg

of $0.08 \pm 0.03 \text{ ‰}$, and $\Delta^{200}\text{Hg}$ of $0.03 \pm 0.04 \text{ ‰}$ (1σ , $n = 57$). Procedural control SRMs NIST1632d (coal, $n = 17$), NIST2685b (coal, $n = 7$), and BCR482 (lichen, $n = 5$) were prepared following the same protocol as peat samples and yielded results with 2σ of 0.16 ‰ on $\delta^{202}\text{Hg}$, 0.06 ‰ on $\Delta^{199}\text{Hg}$. Every sample was measured for Hg isotopic composition in duplicate. Additional measurements were made when duplicate results exceeded 2σ of procedural standards. Results are presented in Tables S5–S8.

Total HgAR Calculation and Mastercore Construction.

Total HgAR was calculated for Estibere peat core using the following formula:

$$\text{HgAR}_{\text{total}} = \frac{c(\text{Hg}) \times \text{thickness} \times \text{density}}{dt} \quad (3)$$

where $c(\text{Hg})$, thickness, and density correspond to Hg concentration, thickness, and density of a peat sample, and dt is the age interval represented by this sample.

For the Pinet record, the three peat cores were combined to obtain a single record (see Figure S8).

Enrichment Factor Nomenclature. In discussing HgAR, and Hg enrichment factors (EF) we adopt the recent nomenclature by Amos et al.¹¹ who reviewed peat and sediment records of Hg. The considered periods are modern times (1990–present), extended 20th century maximum (20Cmax, i.e., the prolonged period of maximum HgAR), preindustrial (1760–1880 CE), prelarge scale mining (<1550 CE). The following associated enrichment factors are discussed: $\text{EF}_{\text{preind}} = 20\text{Cmax HgAR}/\text{preindustrial HgAR}$; $\text{EF}_{\text{alltime}} = 20\text{Cmax HgAR}/\text{premining HgAR}$. In this study, we also use the term preanthropogenic, which refers to pre-1000 BCE period and predates large changes in land use in Europe.²⁸

RESULTS AND DISCUSSION

Hg Accumulation Rates. The reconstructed Hg accumulation rates ($\text{HgAR}_{\text{total}}$, including both Hg wet deposition and GEM uptake) at Pinet increase from $1.5 \pm 1.0 \mu\text{g m}^{-2} \text{y}^{-1}$ over the period 8000–1000 BCE to $6.5 \pm 2.4 \mu\text{g m}^{-2} \text{y}^{-1}$ during the preindustrial period (1760–1880 CE) (Figure 1A, Table 1). The 20th century maximum HgAR (20Cmax) of $42 \pm 6 \mu\text{g m}^{-2} \text{y}^{-1}$ occurs from 1971–2001 (Table 1). This corresponds to “alltime” ($\text{HgAR}_{20\text{Cmax}}/\text{HgAR}_{<1000\text{BCE}}$) and preindustrial ($\text{HgAR}_{20\text{Cmax}}/\text{HgAR}_{1760-1880\text{CE}}$) enrichment factors, $\text{EF}_{\text{alltime}}$ of 26 ± 4 and $\text{EF}_{\text{preind}}$ of 6 ± 1 , in good agreement with global peat bog $\text{EF}_{\text{alltime}}$ of 27 ± 14 and $\text{EF}_{\text{preind}}$ of 6 ± 4 (1σ , $n = 14$) and lake sediment $\text{EF}_{\text{alltime}}$ of 17 ± 17 and $\text{EF}_{\text{preind}}$ of 3 ± 1 (1σ , $n = 7$).¹¹ The historical evolution of HgARs inferred from the Estibere peat core reveals a gradual increase from $2.4 \pm 0.5 \mu\text{g m}^{-2} \text{y}^{-1}$ in the Middle Ages (800–1500 CE) to $6.0 \pm 1.3 \mu\text{g m}^{-2} \text{y}^{-1}$ during preindustrial times (1760–1880 CE), reaching $24 \pm 2 \mu\text{g m}^{-2} \text{y}^{-1}$ ($\text{EF}_{\text{preind}} = 4 \pm 1$) during the Estibere 20Cmax (1946–1974 CE) and decreasing to $9.2 \pm 3.5 \mu\text{g m}^{-2} \text{y}^{-1}$ in 1990–2011 CE (Figure 1A, Table 1). The timing of the Estibere 20Cmax period is therefore in good agreement with other peat studies (mean 20Cmax of 1940–1977 CE),¹¹ while the Pinet 20Cmax period is unusually late (1971–2001 CE).

Hg Stable Isotopes. Hg stable isotopes have proven to efficiently trace sources and processes affecting Hg cycling.²⁹ Because our sites are located far from Hg emission sources, deposited Hg derives from long-range transport, and the Hg isotope source signatures may have been affected by

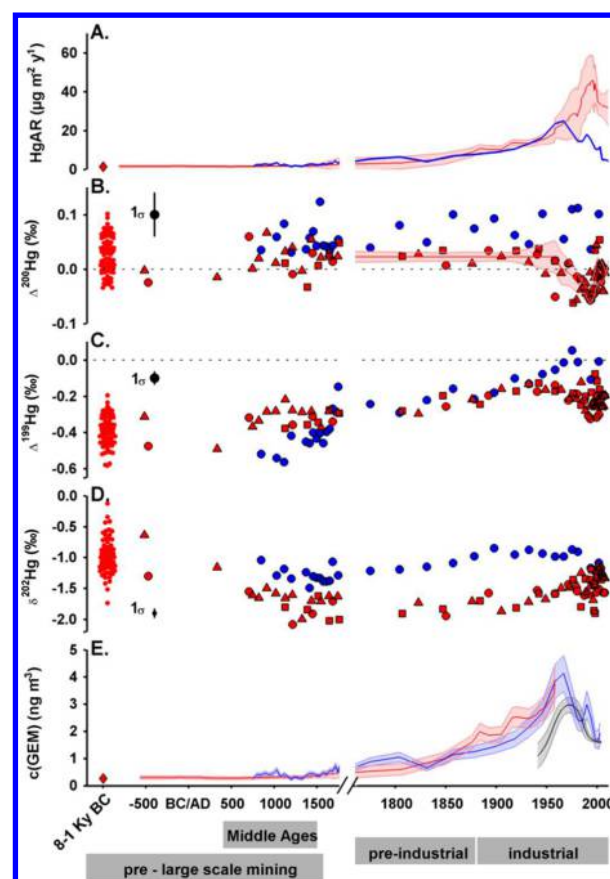


Figure 1. Historical total HgAR (A), peat $\Delta^{200}\text{Hg}$ (B), $\Delta^{199}\text{Hg}$ (C), $\delta^{202}\text{Hg}$ (D), and GEM concentration (E) reconstructed from Estibere peat core (blue lines and circles) and Pinet peat cores (red lines and symbols). Scatters (B, C, D) and red diamonds (A, E) represent Hg isotope variability and averages HgARs and GEM concentration for the period 8000–1000 BCE in Pinet cores. Red ●, ▲ and ■ respectively stand for Pinet cores A, B and C.

atmospheric Hg cycling. All Hg transformations potentially lead to mass-dependent fractionation (MDF) of the seven stable Hg isotopes (mass range 196 to 204). Odd mass Hg isotopes show mass independent isotope fractionation (MIF, $\Delta^{199}\text{Hg}$, $\Delta^{201}\text{Hg}$) during photochemical Hg transformations.^{27,30} Unusual even Hg isotope MIF, producing positive $\Delta^{200}\text{Hg}$ and negative $\Delta^{204}\text{Hg}$, has been observed in rainfall Hg in N-America, Asia and Europe.^{20,31,32} Even-MIF is thought to be exclusively generated during oxidation of GEM in the upper troposphere and stratosphere.³² At the Earth surface, $\Delta^{200}\text{Hg}$ (and $\Delta^{204}\text{Hg}$) can therefore be used as conservative source tracers in Earth surface ecosystems.^{20,33,34} Our previous study of Hg accumulation by living sphagnum moss and surface peat at Pinet illustrated how $\Delta^{200}\text{Hg}$ (and $\Delta^{204}\text{Hg}$) can be used to identify and quantify GEM dry deposition to sphagnum.²⁰ Jiskra et al.³⁵ suggested that postdepositional dark Hg reduction influenced soil Hg isotope signatures ($\delta^{202}\text{Hg}$ and $\Delta^{199}\text{Hg}$, but not $\Delta^{200}\text{Hg}$). We do not however observe the expected trend for such process in the surface peat layers, suggesting that Hg deposited to sphagnum is preserved in peat.²⁰

Figure 2 shows Hg isotope variability ($\delta^{202}\text{Hg}$, $\Delta^{199}\text{Hg}$, and $\Delta^{200}\text{Hg}$) in local rainfall and GEM in the Pyrenees and in the Pyrenean peat cores. Similar to living vegetation and surface peat,^{20,36} the down-core peat $\delta^{202}\text{Hg}$ enrichment in the lighter isotopes by foliar GEM uptake, and peat $\Delta^{200}\text{Hg}$ similarity to

Table 1. Summary of the Results for Pinet and Estibere Peatlands

	preanthropogenic	middle ages	preindustrial	20Cmax	modern
Pinet peat bog					
age interval	8000–1000 BCE	500–1500 CE	1760–1880 CE	1971–2001 CE	2001–2011 CE
HgAR _{total} ($\mu\text{g m}^{-2} \text{y}^{-1}$)	1.5 ± 1.0	1.7 ± 0.1	6.5 ± 2.4	40 ± 6	29 ± 3
HgAR _{wet} ($\mu\text{g m}^{-2} \text{y}^{-1}$)	0.4 ± 0.2	0.46 ± 0.02	1.8 ± 0.7	5.1 ± 2.9^a	4.5 ± 0.9^a
HgAR _{dry} ($\mu\text{g m}^{-2} \text{y}^{-1}$)	1.1 ± 0.4	1.22 ± 0.07	4.7 ± 1.8	36 ± 7	24 ± 2
V_{GEM} (cm s^{-1})	0.013 ± 0.004	0.013 ± 0.004	0.013 ± 0.004		0.050 ± 0.005
$c(\text{GEM})$ (ng m^{-3})	0.27 ± 0.11	0.31 ± 0.02	1.2 ± 0.4		
Estibere peatland					
age interval		800–1500 CE	1760–1880 CE	1946–1967 CE	1990–2011 CE
HgAR _{total} ($\mu\text{g m}^{-2} \text{y}^{-1}$)		2.4 ± 0.5	6.0 ± 1.3	24 ± 2	9.2 ± 3.5
HgAR _{wet} ($\mu\text{g m}^{-2} \text{y}^{-1}$)		1.1 ± 0.3	2.6 ± 0.6	11 ± 1	4.0 ± 1.5
HgAR _{dry} ($\mu\text{g m}^{-2} \text{y}^{-1}$)		1.3 ± 0.3	3.4 ± 0.8	14 ± 1	5.2 ± 2.0
V_{GEM} (cm s^{-1})		0.011 ± 0.003	0.011 ± 0.003	0.011 ± 0.003	0.011 ± 0.003
$c(\text{GEM})$ (ng m^{-3})		0.38 ± 0.08	1.0 ± 0.2	3.9 ± 0.5	1.5 ± 0.6

^aThe 20Cmax period for HgAR_{wet} is different than for HgAR_{total} at Pinet (see SI). 20Cmax HgAR_{wet} value is for the period 1942–1964 CE, and modern HgAR_{wet} value for the period 1990–2011 CE.

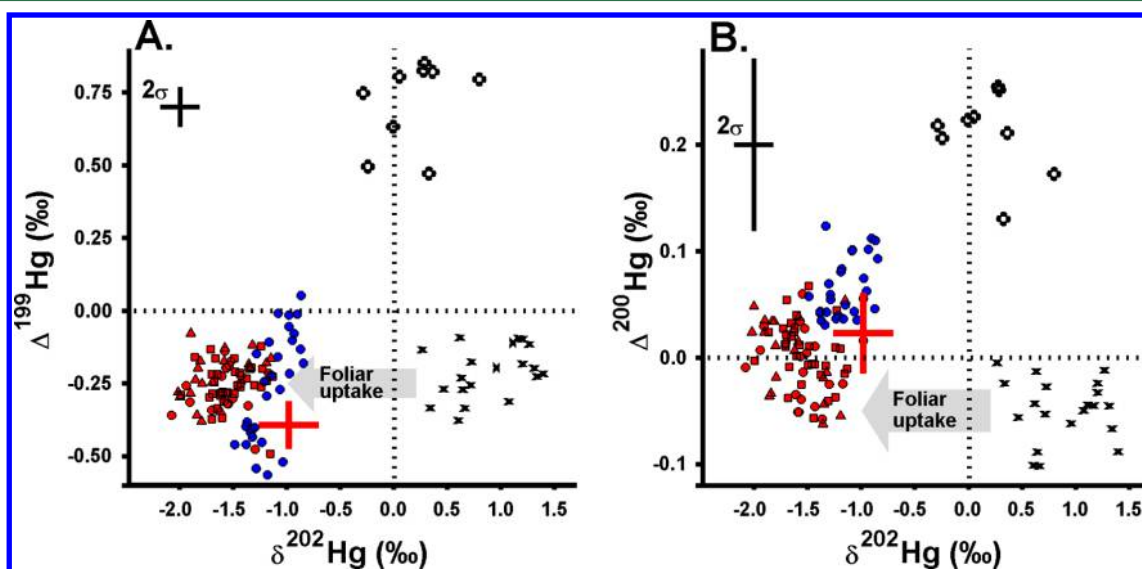


Figure 2. $\delta^{202}\text{Hg}$ vs $\Delta^{199}\text{Hg}$ (A), and $\Delta^{200}\text{Hg}$ (B) signatures in atmospheric gaseous Hg (x), Hg wet deposition (O) and post-1000 BCE Pinet (red \blacktriangle , red \blacksquare , red \bullet) and Estibere (blue \bullet) peat cores. Red crosses represent the mean $\pm 1\sigma$ of Holocene Pinet peat ($n = 77$).

the GEM pool suggests GEM dry deposition to have been the dominant Hg accumulation mechanism in Pyrenean peat bogs throughout the Holocene (see SI and Figure S9). Estibere peat systematically displays higher $\Delta^{200}\text{Hg}$ ($0.06 \pm 0.03 \text{‰}$, 1σ , $n = 29$, period 800–2011 CE) than Pinet peat ($0.01 \pm 0.04 \text{‰}$, 1σ , $n = 149$, period 8000 BCE to 2011 CE), reflecting a slightly larger contribution from Hg wet deposition (Figure 2). Indeed, annual precipitation at Estibere (1400 mm, 2300 m altitude) is higher than at Pinet (1161 mm, 880 m altitude). Using present-day Pinet rainfall $\Delta^{200}\text{Hg}$ ($0.21 \pm 0.04 \text{‰}$, 1σ , $n = 9$) and GEM $\Delta^{200}\text{Hg}$ ($-0.05 \pm 0.02 \text{‰}$, 1σ , $n = 10$) as end-members we estimate past GEM dry deposition (HgAR_{dry}) and Hg wet deposition (HgAR_{wet}) to Pinet and Estibere bogs using a mass balance approach (Figures 1B and S10). The calculated mean GEM dry deposition contributions to HgAR are $57 \pm 8\%$ at Estibere and $77 \pm 8\%$ at Pinet (both 1σ , $n = 29$ and 149, respectively). The validity of these estimates depends critically on whether GEM and rainfall $\Delta^{200}\text{Hg}$ have remained constant over the Holocene. Extensive work on volcanic and coal Hg contents and emissions (summarized in Sun et al., 2016³⁷)

shows identical near-zero $\Delta^{200}\text{Hg}$ in both volcanic (0.03‰) and coal (0.01‰) Hg emission sources. There is therefore no reason to suspect that past noncoal Hg emissions, whether volcanic or anthropogenic (other than coal), led to changing $\Delta^{200}\text{Hg}$ emissions over the past 10 000 years. A study reporting Hg isotope signatures in ice cores did not reveal any change in $\Delta^{200}\text{Hg}$ during industrialization, confirming the hypothesis of constant $\Delta^{200}\text{Hg}$ signatures in the atmosphere.³⁸ The Estibere and Pinet (8000 BCE to 1970 CE) $\Delta^{200}\text{Hg}$ profiles do not reveal significant variability (Figure 1B), suggesting that the relative proportions of GEM dry deposition and Hg wet deposition to the bogs did not change through time. This observed constancy of Pinet and Estibere $\Delta^{200}\text{Hg}$ records supports our assumption of constant GEM and rainfall $\Delta^{200}\text{Hg}$ over time as it would be highly unlikely that temporally varying $\Delta^{200}\text{Hg}$ sources contributed to yield constant $\Delta^{200}\text{Hg}$ GEM and rainfall pools over time.

In all three Pinet records, a significant decrease in $\Delta^{200}\text{Hg}$ occurs however around 1970, suggesting that GEM dry deposition became more important during the last 40 years

(average $89 \pm 8\%$ for 1970–2010 period, 1σ , $n = 37$) compared to the pre-1970 period ($74 \pm 7\%$ from 8000 BCE to 1970 CE, 1σ , $n = 112$; t test $p < 0.05$). Consequently, a difference in HgAR_{dry} between the two peatlands is observed during the industrial period (Figure S10), with a late peak in HgAR_{dry} at Pinet (1971–2001 CE) compared to Estibere (1946–1967). This late peak in the Pinet record coincides with the deliberate, partial draining of the peat bog (by a 10 m wide, 2 m deep ditch, 75 m from the coring sites), and concomitant onset of changes in hydrology and vegetation cover.³⁹ Even-MIF at Pinet is therefore a sensitive tracer of ecosystem changes. GEM dry deposition is thought to predominantly reflect GEM uptake by sphagnum foliage.²⁰ We suggest that the GEM uptake rate by sphagnum increased after the partial draining (see SI). This indicates that in addition to Hg wet deposition and atmospheric GEM concentration, peatland ecology also partly controls peat HgARs. Peat Hg isotope signatures are therefore useful to distinguish the variations in HgARs related to atmospheric processes from those related to peat bog ecology.

Reconstructing Past GEM. The reconstruction of past GEM concentrations requires knowledge of both HgAR_{dry} ($\mu\text{g m}^{-2} \text{y}^{-1}$) and the net annual GEM dry deposition velocity (V_{GEM} in cm s^{-1}), where $\text{GEM} = \text{HgAR}_{\text{dry}}/V_{\text{GEM}}$. We estimate V_{GEM} using GEM dry deposition estimates from recent peat layers (HgAR_{dry} of 29 ± 3 and $5.2 \pm 2.0 \mu\text{g m}^{-2} \text{y}^{-1}$ for Pinet and Estibere, respectively) and modern GEM concentrations monitored over Europe ($1.5 \pm 0.3 \text{ ng m}^{-3}$, 1σ , period 1990–2011¹⁷). We obtain a modern V_{GEM} of $0.050 \pm 0.005 \text{ cm s}^{-1}$ for the Pinet peat bog and $0.011 \pm 0.003 \text{ cm s}^{-1}$ for Estibere, which lie within the range of field observations over vegetated ecosystems.⁴⁰ The Estibere $\Delta^{200}\text{Hg}$ profile does not vary over the Holocene, implying that V_{GEM} remained constant. We therefore extrapolate Estibere V_{GEM} for the modern period to deeper peat layers and estimate mean GEM concentrations of $0.38 \pm 0.08 \text{ ng m}^{-3}$ during the Middle Ages (800–1550 CE), increasing to $1.0 \pm 0.2 \text{ ng m}^{-3}$ during preindustrial times (1550–1780 CE), reaching a maximum of $3.9 \pm 0.5 \text{ ng m}^{-3}$ from 1946–1967, and leveling off to $1.5 \pm 0.6 \text{ ng m}^{-3}$ from 1990–2011.

At Pinet, variations in $\Delta^{200}\text{Hg}$ indicated a change in dry/wet HgAR contributions over the past ~40 years (Figure 1B), probably related to variations in V_{GEM} due to the partial draining of the peat bog in the 1970's. Because of this ecological change at the Pinet peat bog surface, present-day V_{GEM} cannot be applied to deeper peat layers. However, we can use GEM concentrations reconstructed from the Estibere record for the period 800–1970 (Figure 1E) and HgAR_{dry} from Pinet cores for the same period (Table 1) to estimate a pre-1970 V_{GEM} for the Pinet peat bog ($0.013 \pm 0.004 \text{ cm s}^{-1}$). The resulting pre-1970 V_{GEM} can then be applied to deeper Holocene Pinet peat layers in order to reconstruct a mean preanthropogenic (8000–1000 BCE) GEM concentration of $0.27 \pm 0.11 \text{ ng m}^{-3}$. The Holocene GEM level of 0.3 ng m^{-3} is the first ever archive-based reconstruction of what atmospheric Hg levels may have been during preanthropogenic times. Figure 3 shows that reconstructed Estibere GEM levels since 1940 are consistent with (1) the single historical GEM reconstruction for the period 1940–2000 CE based on GEM measurements in polar firn air,¹⁸ which gave a maximum GEM concentration of $3.0 \pm 0.5 \text{ ng m}^{-3}$ around 1970, and (2) global atmospheric Hg monitoring since the 1970s, showing a decline from ~3 ng m^{-3} in 1974–1979 to 1.5 ng m^{-3} in 1990–2010 (Figure 3). Maximum 20th century GEM levels in the Pyrenees were

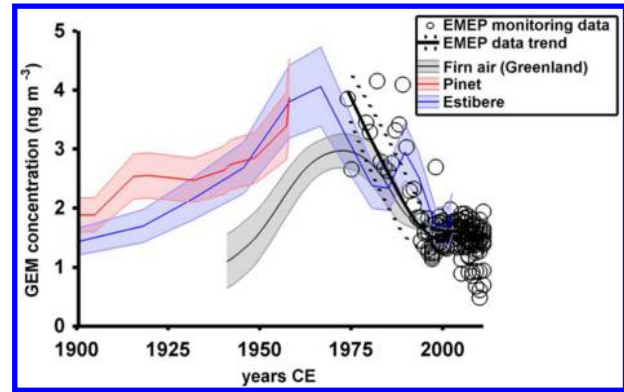


Figure 3. Reconstructed atmospheric GEM concentrations from Pinet (1900–1970 CE) and Estibere (1900–2011 CE) peat cores, compared to monitored concentrations across Europe (EMEP), and GEM concentration reconstructed from polar firn air in Greenland (after Fain et al., 2009¹⁸).

15 ± 4 times higher than reconstructed Holocene GEM levels and suggest that human impacts on global atmospheric Hg levels are larger than the factor of 3 ± 1 previously thought.

Historical Variations in Peat Hg Isotope Signatures. Downcore peat $\delta^{202}\text{Hg}$ and $\Delta^{199}\text{Hg}$ variations represent historical changes in Hg emission sources to the atmosphere and/or changes in Earth surface Hg isotope fractionation processes. Historical peat $\delta^{202}\text{Hg}$ variations at Pinet show a pronounced -0.7 ‰ shift (t test $p < 0.05$) between preanthropogenic ($-0.98 \pm 0.28 \text{ ‰}$, 1σ , $n = 76$, 8000–1000 BCE) and medieval peat layers ($-1.72 \pm 0.17 \text{ ‰}$, 1σ , $n = 15$, 500–1500 CE). This decreasing trend in $\delta^{202}\text{Hg}$ is also reflected in the single Estibere peat core from 800 CE ($\delta^{202}\text{Hg} = -1.17 \pm 0.12$, 1σ , $n = 3$, period 800–1100 CE), reaching a minimum of $-1.38 \pm 0.01 \text{ ‰}$ (1σ , $n = 3$, period 1450–1530 CE) around 1500 CE (t test $p < 0.05$) (Figure 1). The shift in Pinet peat $\delta^{202}\text{Hg}$ is accompanied by near constant $\Delta^{199}\text{Hg}$ of $-0.39 \pm 0.08 \text{ ‰}$ (1σ , $n = 76$) in 8000–1000 BCE to $-0.32 \pm 0.05 \text{ ‰}$ (1σ , $n = 15$) in 500–1500 CE (constant although t test $p < 0.05$ indicates a slight increase). Although Estibere $\Delta^{199}\text{Hg}$ increases during the Middle Ages, its mean value remains similar to Holocene $\Delta^{199}\text{Hg}$. The key feature of the Pinet record, i.e., the -0.7 ‰ $\delta^{202}\text{Hg}$ shift predates Spanish colonial mining (1570–1820 CE), which potentially emitted large amounts of Hg to the atmosphere.⁴¹ Medieval mining and metallurgy could have had an influence on atmospheric Hg locally, yet does not have low enough $\delta^{202}\text{Hg}$ (-0.6 ‰ for cinnabar and -0.5 ‰ for Zn ores)³⁷ to support the observations. The only plausible Hg emission source which would induce the observed trends in peat $\delta^{202}\text{Hg}$, $\Delta^{199}\text{Hg}$ and reconstructed GEM during the medieval period is biomass burning, since it would emit Hg with low $\delta^{202}\text{Hg}$, and with $\Delta^{199}\text{Hg}$ similar to concurrent GEM (i.e., at 1000 CE). European deforestation, as inferred from population dynamics, has indeed been extensive since 1000 BCE.²⁸ In addition, deforestation associated with land use change limits foliar sequestration of GEM and may have resulted in regionally higher GEM levels with lesser enrichment in heavy Hg isotopes (lower $\delta^{202}\text{Hg}$). We therefore suggest that the medieval decrease in $\delta^{202}\text{Hg}$ and minor increase in reconstructed GEM levels (insignificant considering uncertainties, see Table 1) was caused by biomass burning and the negative feedback that deforestation had on foliar GEM sequestration.

The first large increase in GEM concentration (factor of 3–4 compared to preanthropogenic times) starts around 1500 CE in the Estibere and Pinet records and reaches 1.0–1.2 ng m⁻³ during the preindustrial period (1750–1880 CE; Table 1), which suggests a new important Hg emission source. Other European records also display increasing HgARs in this period.^{8,42–44} The increase in HgAR has been suggested to represent Hg extraction for silver and gold amalgamation since the 16th century.^{11,45} The absence of pronounced change in both $\delta^{202}\text{Hg}$ and $\Delta^{199}\text{Hg}$ at Estibere and Pinet over the European Renaissance period (1500–1750 CE) suggest, however, little change in Hg emission sources, i.e. continued biomass burning driven by population dynamics.

In both Estibere and Pinet cores, reconstructed GEM, $\delta^{202}\text{Hg}$, and $\Delta^{199}\text{Hg}$ do gradually increase during the preindustrial and industrial periods (1750–2010 for Estibere; 1750–1970 for Pinet due to ecological disturbance >1970) by 3 ng m⁻³, 0.3 ‰ and 0.15 ‰, respectively (Figure 1C–E). Similar increases in $\delta^{202}\text{Hg}$ and $\Delta^{199}\text{Hg}$ during the industrial period were observed in lake sediment studies.^{46–50} The increase in $\delta^{202}\text{Hg}$ partly parallels a recently estimated 0.4 ‰ increase in the $\delta^{202}\text{Hg}$ of bulk anthropogenic Hg emissions from 1850 to 2010 and reflects a shift in Hg emissions from the mining to energy sectors.³⁷ However, the observed increase in $\Delta^{199}\text{Hg}$ is not compatible with the Hg isotope emission inventory as both natural and anthropogenic Hg emission sources carry near-zero $\Delta^{199}\text{Hg}$.³⁷ Modern day negative atmospheric $\Delta^{199}\text{Hg}_{\text{GEM}}$ is counterbalanced by positive rainfall $\Delta^{199}\text{Hg}$, representative of atmospheric oxidized Hg species (Figure 2). This careful balance results from ill-identified atmospheric photochemical Hg redox transformations. The temporal change in peat $\Delta^{199}\text{Hg}$ over the past millennium suggests that the regional or possibly global atmospheric Hg redox balance has changed. Alternatively, the broad shift from medieval biomass burning emissions with low $\Delta^{199}\text{Hg}$ to industrial emissions with near-zero $\Delta^{199}\text{Hg}$ may also play a role. While more work is needed to refine the $\Delta^{199}\text{Hg}$ tracer, our study clearly shows that paleo-Hg isotope records are powerful tools to constrain atmospheric and ecological processes as well as anthropogenic impacts. Our finding that human impacts on atmospheric GEM levels have been larger than previously recognized sets a new benchmark for environmental policy under the UNEP Minamata Convention.

AUTHOR INFORMATION

Corresponding Authors

*Tel. +33 5 61 33 26 06; e-mail: maxime.enrico@get.obs-mip.fr (M.E.).

*E-mail: sonke@get.obs-mip.fr (J.E.S.).

ORCID

Maxime Enrico: 0000-0002-9322-7057

Jeroen E. Sonke: 0000-0001-7146-3035

Present Address

^{||}Aix Marseille Université, CNRS/INSU, Université de Toulon, IRD, Mediterranean Institute of Oceanography (MIO) UM 110, 13288, Marseille, France.

Notes

The authors declare no competing financial interest.

ACKNOWLEDGMENTS

This work was supported by research grants ANR-09-JCJC-0035-01 from the French Agence Nationale de Recherche and ERC-2010-StG_20091028 from the European Research Council to JES. Bruno Le Roux and the Association Aude Claire are thanked for Pinet coring permission and help on the field. Same for Didier Galop and the Pyrenees National Park for Estibère peatland. Frederic Candaudap and David Baqué are thanked for helping with Pb stable isotope analyses.

REFERENCES

- (1) Krabbenhoft, D. P.; Sunderland, E. M. Environmental science. Global change and mercury. *Science* **2013**, *341* (6153), 1457–8.
- (2) Schuster, P. F.; Krabbenhoft, D. P.; Naftz, D. L.; Cecil, L. D.; Olson, M. L.; Dewild, J. F.; Susong, D. D.; Green, J. R.; Abbott, M. L. Atmospheric Mercury Deposition during the Last 270 Years: A Glacial Ice Core Record of Natural and Anthropogenic Sources. *Environ. Sci. Technol.* **2002**, *36* (11), 2303–2310.
- (3) Jitaru, P.; Gabrielli, P.; Marteel, A.; Plane, J. M. C.; Planchon, F. A. M.; Gauchard, P.-A.; Ferrari, C. P.; Boutron, C. F.; Adams, F. C.; Hong, S.; Cescon, P.; Barbante, C. Atmospheric depletion of mercury over Antarctica during glacial periods. *Nat. Geosci.* **2009**, *2* (7), 505–508.
- (4) Fitzgerald, W. F.; Engstrom, D. R.; Lamborg, C. H.; Tseng, C.-M.; Balcom, P. H.; Hammerschmidt, C. R. Modern and Historic Atmospheric Mercury Fluxes in Northern Alaska: Global Sources and Arctic Depletion. *Environ. Sci. Technol.* **2005**, *39* (2), 557–568.
- (5) Engstrom, D. R.; Fitzgerald, W. F.; Cooke, C. A.; Lamborg, C. H.; Drevnick, P. E.; Swain, E. B.; Balogh, S. J.; Balcom, P. H. Atmospheric Hg emissions from preindustrial gold and silver extraction in the Americas: a reevaluation from lake-sediment archives. *Environ. Sci. Technol.* **2014**, *48* (12), 6533–43.
- (6) Cooke, C. A.; Balcom, P. H.; Biester, H.; Wolfe, A. P. Over three millennia of mercury pollution in the Peruvian Andes. *Proc. Natl. Acad. Sci. U. S. A.* **2009**, *106* (22), 8830–4.
- (7) Roos-Barraclough, F.; Martinez-Cortizas, A.; García-Rodeja, E.; Shoty, W. A 14 500 year record of the accumulation of atmospheric mercury in peat: volcanic signals, anthropogenic influences and a correlation to bromine accumulation. *Earth Planet. Sci. Lett.* **2002**, *202* (2), 435–451.
- (8) Martinez-Cortizas, A.; Pontevedra-Pombal, X.; Garcia-Rodeja, E.; Novoa-Munoz, J. C.; Shoty, W. Mercury in a spanish peat bog: archive of climate change and atmospheric metal deposition. *Science* **1999**, *284* (5416), 939–942.
- (9) Bindler, R. Estimating the natural background atmospheric deposition rate of mercury utilizing ombrotrophic bogs in southern Sweden. *Environ. Sci. Technol.* **2003**, *37* (1), 40–6.
- (10) Amos, H. M.; Jacob, D. J.; Streets, D. G.; Sunderland, E. M. Legacy impacts of all-time anthropogenic emissions on the global mercury cycle. *Global Biogeochem. Cycles* **2013**, *27* (2), 410–421.
- (11) Amos, H. M.; Sonke, J. E.; Obrist, D.; Robins, N.; Hagan, N.; Horowitz, H. M.; Mason, R. P.; Witt, M.; Hedgecock, I. M.; Corbitt, E. S.; Sunderland, E. M. Observational and modeling constraints on global anthropogenic enrichment of mercury. *Environ. Sci. Technol.* **2015**, *49* (7), 4036–47.
- (12) Lyman, S. N.; Jaffe, D. A. Formation and fate of oxidized mercury in the upper troposphere and lower stratosphere. *Nat. Geosci.* **2011**, *5* (2), 114–117.
- (13) Lindberg, S.; Bullock, R.; Ebinghaus, R.; Engstrom, D.; Feng, X.; Fitzgerald, W.; Pirrone, N.; Prestbo, E.; Seigneur, C. A synthesis of

progress and uncertainties in attributing the sources of mercury in deposition. *Ambio* **2007**, *36* (1), 19–32.

(14) Schroeder, W. H.; Anlauf, K. G.; Barrie, L. A.; Lu, J. Y.; Steffen, A.; Schneeberger, D. R.; Berg, T. Arctic springtime depletion of mercury. *Nature* **1998**, *394* (6691), 331–332.

(15) Obrist, D.; Tas, E.; Peleg, M.; Matveev, V.; Fain, X.; Asaf, D.; Luria, M. Bromine-induced oxidation of mercury in the mid-latitude atmosphere. *Nat. Geosci.* **2011**, *4* (1), 22–26.

(16) Lamborg, C. H.; Hammerschmidt, C. R.; Bowman, K. L.; Swarr, G. J.; Munson, K. M.; Ohnemus, D. C.; Lam, P. J.; Heimburger, L. E.; Rijkenberg, M. J.; Saito, M. A. A global ocean inventory of anthropogenic mercury based on water column measurements. *Nature* **2014**, *512* (7512), 65–8.

(17) EMEP European Monitoring and Evaluation Programme. <http://www.emep.int/> (accessed on 9/15/2016).

(18) Fain, X.; Ferrari, C. P.; Dommergue, A.; Albert, M. R.; Battle, M.; Severinghaus, J.; Arnaud, L.; Barnola, J. M.; Cairns, W.; Barbante, C.; Boutron, C. Polar firn air reveals large-scale impact of anthropogenic mercury emissions during the 1970s. *Proc. Natl. Acad. Sci. U. S. A.* **2009**, *106* (38), 16114–9.

(19) Lamborg, C. H.; Fitzgerald, W. F.; Damman, A. W. H.; Benoit, J. M.; Balcom, P. H.; Engstrom, D. R. Modern and historic atmospheric mercury fluxes in both hemispheres: Global and regional mercury cycling implications. *Global Biogeochem. Cycles* **2002**, *16* (4), 51–1–51–11.

(20) Enrico, M.; Roux, G. L.; Maruszczak, N.; Heimburger, L. E.; Claustres, A.; Fu, X.; Sun, R.; Sonke, J. E. Atmospheric Mercury Transfer to Peat Bogs Dominated by Gaseous Elemental Mercury Dry Deposition. *Environ. Sci. Technol.* **2016**, *50* (5), 2405–12.

(21) Givélet, N.; Le Roux, G.; Cheburkin, A.; Chen, B.; Frank, J.; Goodsite, M. E.; Kempter, H.; Krachler, M.; Noernberg, T.; Rausch, N.; Rheinberger, S.; Roos-Barraclough, F.; Sapkota, A.; Scholz, C.; Shoty, W. Suggested protocol for collecting, handling and preparing peat cores and peat samples for physical, chemical, mineralogical and isotopic analyses. *J. Environ. Monit.* **2004**, *6* (5), 481–92.

(22) Le Roux, G.; De Vleeschouwer, F. Preparation of peat samples for inorganic geochemistry used as palaeoenvironmental proxies. *Mires and Peat* **2010**, *7*, 9.

(23) van Beek, P.; Souhaut, M.; Lansard, B.; Bourquin, M.; Reyss, J. L.; von Ballmoos, P.; Jean, P. LAFARA: a new underground laboratory in the French Pyrenees for ultra low-level gamma-ray spectrometry. *J. Environ. Radioact.* **2013**, *116*, 152–8.

(24) Appleby, P. G.; Nolan, P. J.; Oldfield, F.; Richardson, N.; Higgitt, S. R. ²¹⁰Pb dating of lake sediments and ombrotrophic peats by gamma assay. *Sci. Total Environ.* **1988**, *69* (0), 157–177.

(25) Yafa, C.; Farmer, J. G.; Graham, M. C.; Bacon, J. R.; Barbante, C.; Cairns, W. R.; Bindler, R.; Renberg, I.; Cheburkin, A.; Emons, H.; Handley, M. J.; Norton, S. A.; Krachler, M.; Shoty, W.; Li, X. D.; Martinez-Cortizas, A.; Pulford, I. D.; MacIver, V.; Schweyer, J.; Steinnes, E.; Sjobakk, T. E.; Weiss, D.; Dolgoplova, A.; Kylander, M. Development of an ombrotrophic peat bog (low ash) reference material for the determination of elemental concentrations. *J. Environ. Monit.* **2004**, *6* (5), 493–501.

(26) Sun, R.; Enrico, M.; Heimburger, L. E.; Scott, C.; Sonke, J. E. A double-stage tube furnace–acid-trapping protocol for the pre-concentration of mercury from solid samples for isotopic analysis. *Anal. Bioanal. Chem.* **2013**, *405* (21), 6771–81.

(27) Bergquist, B. A.; Blum, J. D. Mass-dependent and -independent fractionation of Hg isotopes by photoreduction in aquatic systems. *Science* **2007**, *318* (5849), 417–20.

(28) Kaplan, J. O.; Krumhardt, K. M.; Zimmermann, N. The prehistoric and preindustrial deforestation of Europe. *Quat. Sci. Rev.* **2009**, *28* (27–28), 3016–3034.

(29) Blum, J. D.; Sherman, L. S.; Johnson, M. W. Mercury Isotopes in Earth and Environmental Sciences. *Annu. Rev. Earth Planet. Sci.* **2014**, *42* (1), 249–269.

(30) Zheng, W.; Hintelmann, H. Isotope fractionation of mercury during its photochemical reduction by low-molecular-weight organic compounds. *J. Phys. Chem. A* **2010**, *114* (12), 4246–53.

(31) Gratz, L. E.; Keeler, G. J.; Blum, J. D.; Sherman, L. S. Isotopic composition and fractionation of mercury in Great Lakes precipitation and ambient air. *Environ. Sci. Technol.* **2010**, *44* (20), 7764–70.

(32) Chen, J.; Hintelmann, H.; Feng, X.; Dimock, B. Unusual fractionation of both odd and even mercury isotopes in precipitation from Peterborough, ON, Canada. *Geochim. Cosmochim. Acta* **2012**, *90* (0), 33–46.

(33) Demers, J. D.; Sherman, L. S.; Blum, J. D.; Marsik, F. J.; Dvonch, J. T. Coupling atmospheric mercury isotope ratios and meteorology to identify sources of mercury impacting a coastal urban-industrial region near Pensacola, Florida, USA. *Global Biogeochem. Cycles* **2015**, *29* (10), 1689–1705.

(34) Chen, J.; Hintelmann, H.; Zheng, W.; Feng, X.; Cai, H.; Wang, Z.; Yuan, S.; Wang, Z. Isotopic evidence for distinct sources of mercury in lake waters and sediments. *Chem. Geol.* **2016**, *426*, 33–44.

(35) Jiskra, M.; Wiederhold, J. G.; Skyllberg, U.; Kronberg, R. M.; Hajdas, I.; Kretzschmar, R. Mercury deposition and re-emission pathways in boreal forest soils investigated with Hg isotope signatures. *Environ. Sci. Technol.* **2015**, *49* (12), 7188–96.

(36) Demers, J. D.; Blum, J. D.; Zak, D. R. Mercury isotopes in a forested ecosystem: Implications for air-surface exchange dynamics and the global mercury cycle. *Global Biogeochem. Cycles* **2013**, *27* (1), 222–238.

(37) Sun, R.; Streets, D. G.; Horowitz, H. M.; Amos, H. M.; Liu, G.; Perrot, V.; Toutain, J.-P.; Hintelmann, H.; Sunderland, E. M.; Sonke, J. E. Historical (1850–2010) mercury stable isotope inventory from anthropogenic sources to the atmosphere. *Elementa: Science of the Anthropocene* **2016**, *4*, 000091.

(38) Zdanowicz, C. M.; Krümmel, E. M.; Poulain, A. J.; Yumvihoze, E.; Chen, J.; Štok, M.; Scheer, M.; Hintelmann, H. Historical variations of mercury stable isotope ratios in Arctic glacier firn and ice cores. *Global Biogeochem. Cycles* **2016**, *30* (9), 1324–1347.

(39) Le Roux, B. In *Peat in Horticulture and the Rehabilitation of Mires after Peat Extraction: Which Issues for Tomorrow?* International Conference - Peat & Peatlands 2007 Lamoura, Jura, France, 2007; Lamoura, Jura, France, 2007.

(40) Zhang, L.; Wright, L. P.; Blanchard, P. A review of current knowledge concerning dry deposition of atmospheric mercury. *Atmos. Environ.* **2009**, *43* (37), 5853–5864.

(41) Streets, D. G.; Devane, M. K.; Lu, Z.; Bond, T. C.; Sunderland, E. M.; Jacob, D. J. All-time releases of mercury to the atmosphere from human activities. *Environ. Sci. Technol.* **2011**, *45* (24), 10485–91.

(42) Shoty, W.; Goodsite, M. E.; Roos-Barraclough, F.; Givélet, N.; Le Roux, G.; Weiss, D.; Cheburkin, A. K.; Knudsen, K.; Heinemeier, J.; van Der Knaap, W. O.; Norton, S. A.; Lohse, C. Accumulation rates and predominant atmospheric sources of natural and anthropogenic Hg and Pb on the Faroe Islands. *Geochim. Cosmochim. Acta* **2005**, *69* (1), 1–17.

(43) Roos-Barraclough, F.; Shoty, W. Millennial-Scale Records of Atmospheric Mercury Deposition Obtained from Ombrotrophic and Minerotrophic Peatlands in the Swiss Jura Mountains. *Environ. Sci. Technol.* **2003**, *37* (2), 235–244.

(44) Biester, H.; Bindler, R.; Martinez-Cortizas, A.; Engstrom, D. R. Modeling the Past Atmospheric Deposition of Mercury Using Natural Archives. *Environ. Sci. Technol.* **2007**, *41* (14), 4851–4860.

(45) Lacerda, L. D. Global Mercury Emissions from Gold and Silver Mining. *Water, Air, Soil Pollut.* **1997**, *97* (3–4), 209–221.

(46) Gray, J. E.; Pribil, M. J.; Van Metre, P. C.; Borrok, D. M.; Thapalia, A. Identification of contamination in a lake sediment core using Hg and Pb isotopic compositions, Lake Ballinger, Washington, USA. *Appl. Geochem.* **2013**, *29* (0), 1–12.

(47) Gray, J. E.; Van Metre, P. C.; Pribil, M. J.; Horowitz, A. J. Tracing historical trends of Hg in the Mississippi River using Hg concentrations and Hg isotopic compositions in a lake sediment core, Lake Whittington, Mississippi, USA. *Chem. Geol.* **2015**, *395*, 80–87.

(48) Yin, R.; Lepak, R. F.; Krabbenhoft, D. P.; Hurlley, J. P. Sedimentary records of mercury stable isotopes in Lake Michigan. *Elementa: Science of the Anthropocene* **2016**, *4*, 000086.

(49) Yin, R.; Feng, X.; Hurley, J. P.; Krabbenhoft, D. P.; Lepak, R. F.; Kang, S.; Yang, H.; Li, X. Historical Records of Mercury Stable Isotopes in Sediments of Tibetan Lakes. *Sci. Rep.* **2016**, *6*, 23332.

(50) Donovan, P. M.; Blum, J. D.; Yee, D.; Gehrke, G. E.; Singer, M. B. An isotopic record of mercury in San Francisco Bay sediment. *Chem. Geol.* **2013**, *349–350* (0), 87–98.